APEX
504

COMPARISON OF BULK SHIELDING REACTOR CENTERLINE MEASUREMENTS IN WATER WITH PREDICTIONS

A.W. CASPER

GENERAL ELECTRIC
ATOMIC PRODUCTS DIVISION
AIRCRAFT NUCLEAR PROPULSION DEPARTMENT

ANPD

Printed in USA, Price $1.00. Available from the

Office of Technical Services
U.S. Department of Commerce
Washington 25, D.C.

APEX-504
UC-34 Physics and Mathematics
TID-4500 (14th Edition)

COMPARISON OF BULK SHIELDING REACTOR CENTERLINE MEASUREMENTS IN WATER WITH PREDICTIONS

A. W. Casper

Nuclear Development Laboratories Sub-Section

November 1958

United States Air Force — Contract No. AF 33(600)-38062

United States Atomic Energy Commission — Contract No. AT (11-1)-171

GENERAL ELECTRIC
ATOMIC PRODUCTS DIVISION
AIRCRAFT NUCLEAR PROPULSION DEPARTMENT
Cincinnati 15, Ohio

Published by
Technical Publications Sub-Section
July 1959

Abstract

Measurements of fast neutron and gamma ray dose rates in water along the centerline of the Bulk Shielding Reactor (BSR) are compared with predictions made by use of three available computer programs. It is found that the predictions are very dependent on the assumptions made concerning power distribution and that the more accurate descriptions of the source lead to predictions that agree with measurements to within 20 percent throughout thickness ranges as great as 100 centimeters of water.

Comparison of Bulk Shielding Reactor Centerline Measurements in Water With Predictions

INTRODUCTION

Measurements of fast neutron and gamma ray dose rates[1] are compared with the predictions of point-kernel computation programs 04-1, 04-2, and 14-0.[6] These three programs provide a variety of source descriptions. The source description used in each program is given. Buildup, cross sections, and conversion factors which were employed are also listed. In the gamma dose predictions the secondary gamma dose rate from water is added to the core gamma dose rate.

The gamma-ray point-kernel method used consists, briefly, of combining source-point to receiver-point attenuation with Nuclear Development Corporation of America (NDA) build-up factors summed over energy and source volume. These programs are based on the assumption that the gamma ray attenuation between a source point and a receiver point can be described by a function of the form

$$\Psi(E_j) = B(X_j, E_j) \cdot \epsilon^{-X_j} \tag{1}$$

where $X_j = \Sigma(\mu_j t)$. The function $\Psi(E_j)$ is the attenuation of gamma rays of the *j*-th energy group, and $\Sigma(\mu_j t)$ represents the sum of the relaxation lengths in the path.

The total gamma ray energy flux at a given point is then computed for cylindrical source volumes as

$$\Phi_\gamma = \sum_{j=1}^{J} \frac{CB_j}{4\pi} \int p(Z)\, dZ \int r\, p(r)\, dr \int \frac{\Psi(E_j)}{\rho^2}\, d\phi \tag{2}$$

where the integration is carried out over the entire volume of the core. (For noncylindrical sources the integration is also carried out over the entire core volume, but the form of the volume integral is modified appropriately.) The summation indicated is over energy groups; B_j is the source strength for the *j*-th energy group in Mev/cm^3-watt at the point of maximum power in the core; p(Z) and p(r) are functions describing the power distribution in the core; ρ is the distance between source and detector points; and Ψ has the form given in equation (1).

The gamma dose rate measurements[1] were expressed in ergs/$g_{graphite}$-hr-watt. The conversion factors used to convert the point-kernel dimensions to those employed in the measurements are listed on page 24. They were obtained by multiplying the mass energy absorption coefficients for graphite[5] by the factor 5.76×10^{-3} $\dfrac{\text{ergs/hr}}{\text{Mev/sec}}$.

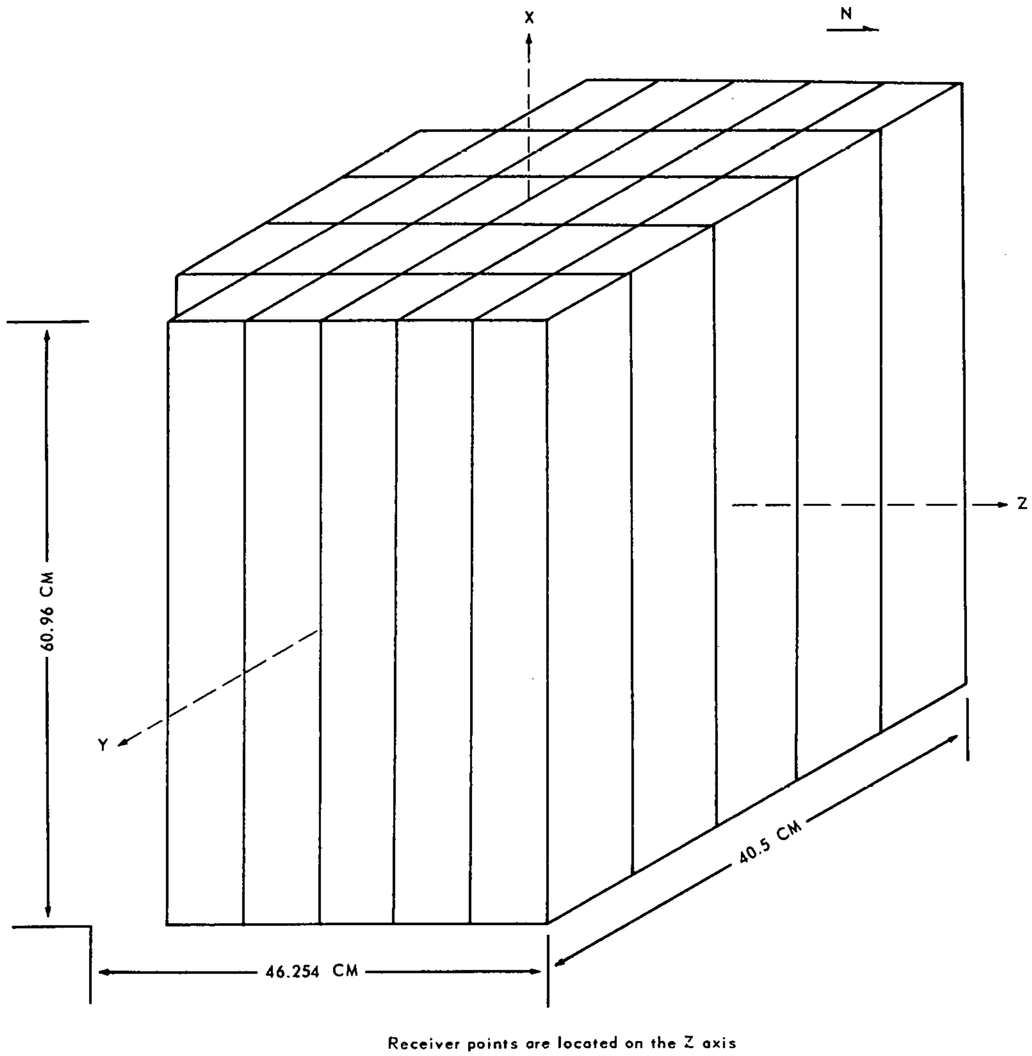

Fig. 1 – Schematic representation of the Bulk Shielding Reactor, loading number 33

The source-point to receiver-point material attenuation function used for fast neutrons in these programs is

$$\Psi_n(\theta,\rho) = 7.29 \times 10^9 \left(\rho \sum_{m=1}^{L} \eta_m \theta_m\right)^{0.29} \exp\left\{-0.83 \left(\rho \sum_{m=1}^{L} \eta_m \theta_m\right)^{0.58}\right\} \exp\left(-\rho \sum_{m=1}^{M} \theta_m \Sigma_m\right). \qquad (3)$$

This function yields dose rates in units of mrep/hr-watt. η_m is the ratio of the hydrogen atom density in material m to that in 70°F water. L refers to the hydrogenous materials among the M materials. The distance from the source point to the receiver point is designated by ρ ; θ_m is the volume fraction of material m; and Σ_m is the fast neutron removal cross section for the nonhydrogenous portion of material m.

The fast neutron dose rate from an entire source region is given by

$$D_n = \int_{\substack{\text{source}\\ \text{region}}} \frac{S(\vec{r}_s)\,\Psi_n(\theta,\rho)}{4\pi\rho^2}\, dV_s.$$

The manner of integration depends on the source description. The geometric attenuation is given by the function $1/4\pi\rho^2$. The source strength at each point within the source volume is given by $S(\vec{r}_s)$. Equation (3) describes the function $\Psi_n(\theta,\rho)$.

The measured fast neutron dose rates were expressed in ergs/g_{tissue}-hr-watt. The measured values were converted to the dimensions used in the point-kernel programs by the conversion factor,

$$1 \text{ rep/hr-watt} = 93 \text{ ergs}/g_{tissue} - \text{hr} - \text{watt}.$$

SOURCE DESCRIPTIONS

Available information[2] about power distribution in the BSR is in the form of histograms for the Y and Z coordinates. The variation in power in the X direction is described as continuous. The reactor and the fuel elements are treated as rectangular in shape as shown in Figure 1.

Program 04-1 permits a rectangular core description. The missing fuel elements in the rectangular array are described as having zero power. Option 1 in the program was used in an early attempt to describe the power distribution as a continuous function in all three variables. The use of this option led to a difference of 100 percent or greater between measured and predicted values of gamma dose. Option 2 in program 04-1 makes it possible to use the given BSR information in an accurate description of the power distribution. In this option the reactor is described in the input data by means of a table of values of power density at 504 points in one-fourth of the core. When this option was used, the difference between measured and predicted values of gamma dose was less than 40 percent of the measured values for receiver points at distances greater than 20 centimeters from the reactor. It is clear that small differences in source power distribution lead to large differences in gamma dose rate in this problem.

The power density values used in option 2 of program 04-1 are listed in Table 1. Power density values associated with the 504 points used in describing one-fourth of the reactor core are given. The dimensions of the core are X = – 30.48 to 30.48 centimeters, Y = – 20.25 to 20.25 centimeters, and Z = – 23.127 to 23.127 centimeters. Dose rates were calculated at receiver points in the water between Z = 29.777 centimeters and Z = 150 centimeters.

In program 04-2, which permits cylindrical source descriptions only, the rectangular source is replaced with an equivalent cylindrical source. The cross section of the cylinder that is considered

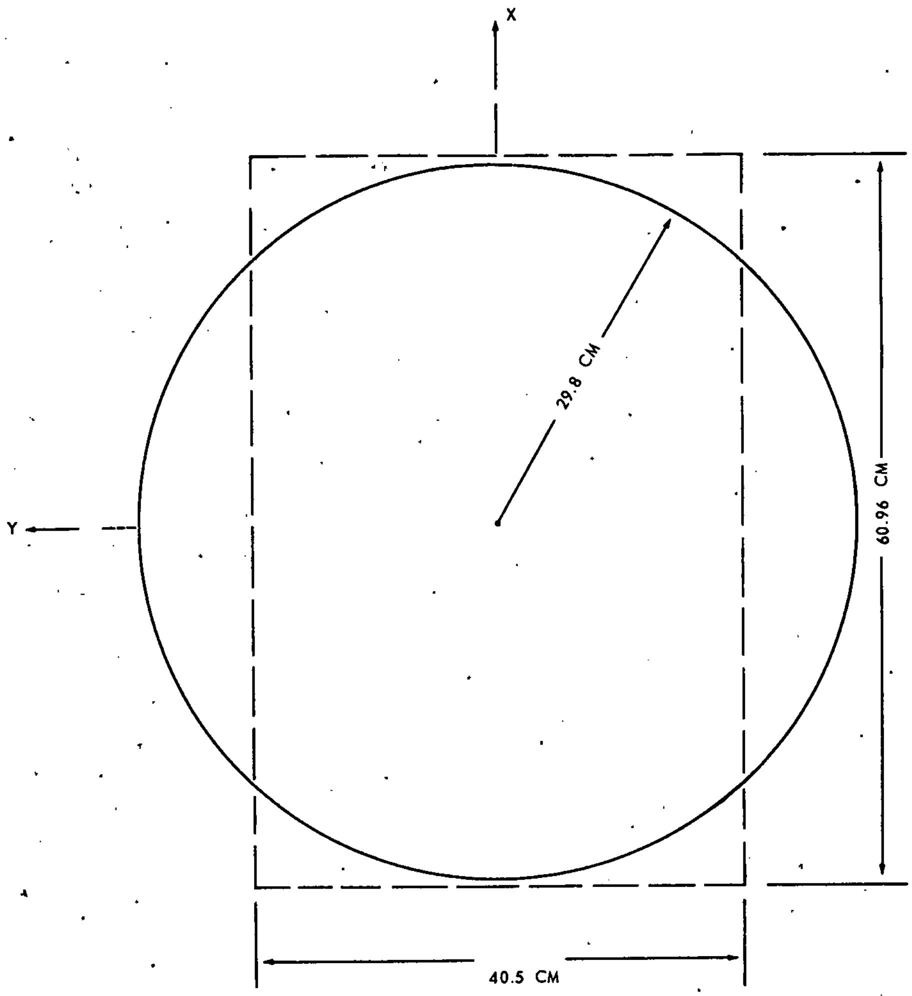

Receiver points are located on the Z axis.

Fig. 2 – Comparison of rectangular-core and cylindrical-core cross sections

to be equivalent to the rectangular cross section of the core is shown in Figure 2. The boundaries of the equivalent cylindrical source are $Z = -20.003$ to 18.097 centimeters and $r = 0$ to 29.8 centimeters. This description makes the volume of the cylinder equal to the volume of the active core. The distribution of power in the equivalent cylindrical source is described with a radial and axial source function. The radial source function used in the program is $P_r = 1 \cdot \cos 0.0374r$. The axial source function used in the program is $P_Z = 1.437 \times 10^{-5} \cos 0.03436 (Z + 4.763)$.

The source distribution is described in program 14-0 as 28 lines. The geometry is indicated in Figure 3. The lines are parallel and located at the center of each fuel element. Points where the lines intersect the X–Y plane are located by the polar coordinates, R and ϕ. The power is assumed to vary along the Z coordinate, and three ranges are used. The lines are divided into six types with a different power description being used for each type. The location of the lines and the power distribution assumed are given in Table 2.

The energy distribution of the gamma source intensity is given in Table 3.

BUILDUP, CROSS SECTIONS, AND CONVERSION FACTORS

The gamma dose buildup, the gamma ray linear absorption cross sections, and the flux-to-dose conversion factors employed in the programs are listed in Tables 4, 5, and 6, respectively. The 04-2 programs used 10 energy groups in the gamma dose predictions. Initial poor results with program 04-1 led to the use of 13 energy groups, but only a small improvement was noted when this change was made. The 13 energy groups are used in the program 04-1 and program 14-0 predictions.

The value 0.0308 per centimeter is used for the neutron removal cross section for oxygen. The uranium and aluminum neutron removal cross sections used are 0.17 per centimeter and 0.079 per centimeter, respectively.

SECONDARY GAMMA RAYS FROM THERMAL NEUTRONS

The source of secondary gamma rays considered here is the 2.23-Mev gamma ray from hydrogen. The thermal neutron cross section used for the (n, γ) reaction is 0.33 barns. Measured values of axial thermal neutron flux are fitted by exponential functions and used as source terms. Measured values from a similar configuration are used to determine radial source functions. The source distribution used is given in Table 7. Water buildup is used. The source was a cylinder 400 centimeters long and 60.96 centimeters in radius. The secondary gamma dose is shown in Figure 4.

GAMMA RAY AND NEUTRON DOSE PREDICTIONS

Neutron dose rates given by programs 04-2, 04-1, and 14-0 are compared with measured values in Figures 5, 6, and 7, respectively. Differences between measured values and predictions near the reactor are noted. The large difference is partly due to widely spaced source points and source points on the surface of the reactor. Program 14-0 has no source points on the reactor surface, and neutron dose rates close to the reactor compare more favorably with measured values in this case.

Gamma dose rates given by programs 04-2, 04-1, and 14-0 are compared with measured values in Figures 8, 9, and 10, respectively. Secondary gamma rays from thermal neutrons are included in the gamma dose predictions. The predicted values agree better with measured values as distances between the reactor and the receiver points increase. This fact is quite clear in Figures 5 and 6 where the source descriptions are better than the description in the program 04-2 problem.

Better agreement between measured and predicted values should be possible by an alteration in the source description. Increasing the number of source points would be one way of improving the source description. However, the value of working for such close agreement should be carefully weighed against cost, inasmuch as the experimental uncertainties in the measurements are as great at 20 percent.[1]

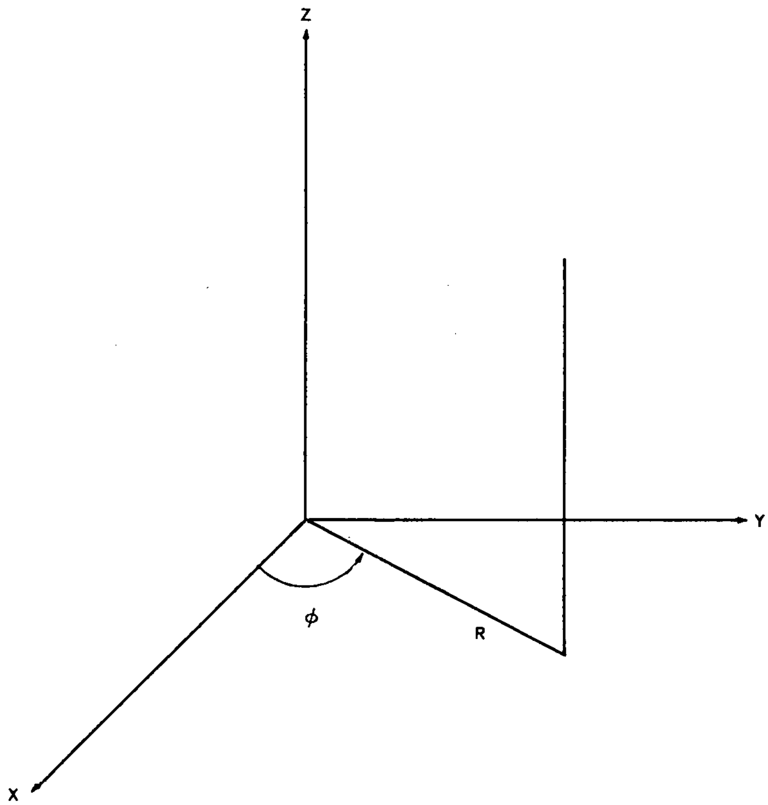

Fig. 3 – Coordinate system used for locating the lines in program 14-0 source description

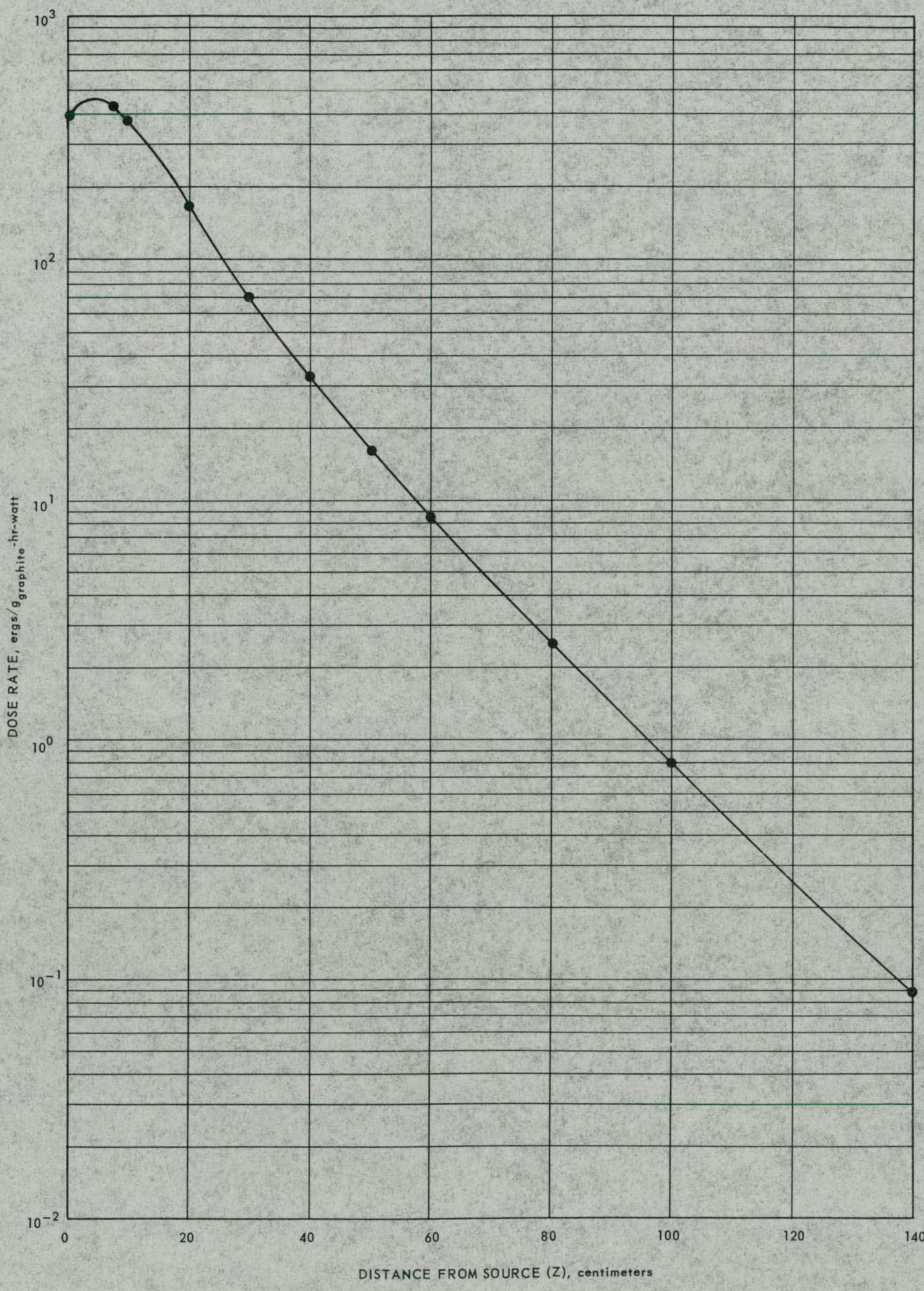

Fig. 4 – Bulk Shielding Reactor centerline secondary gamma dose rate in water, loading number 33

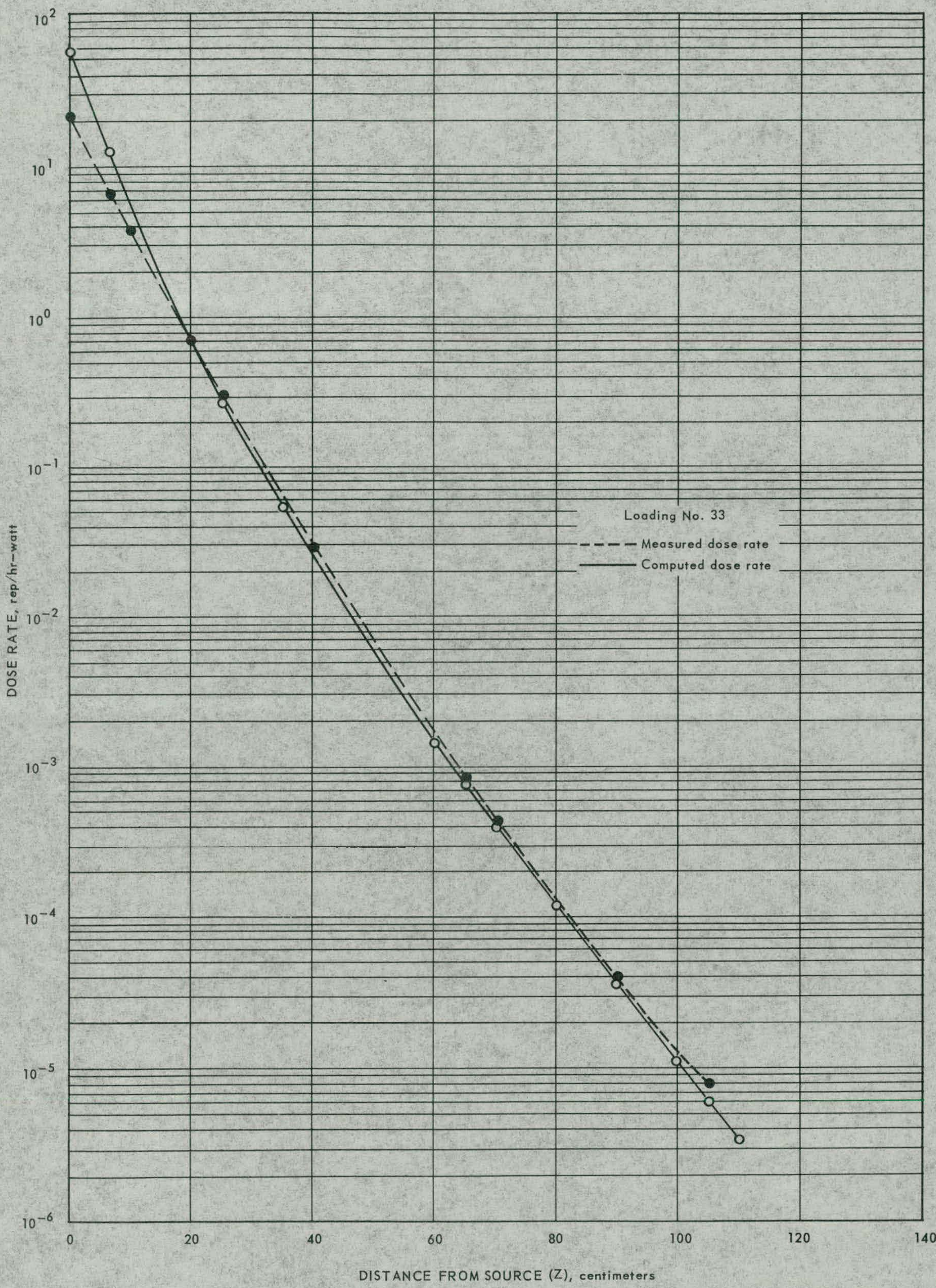

Fig. 5 – Comparison of measured and computed program 04-2 BSR centerline neutron dose rates in water

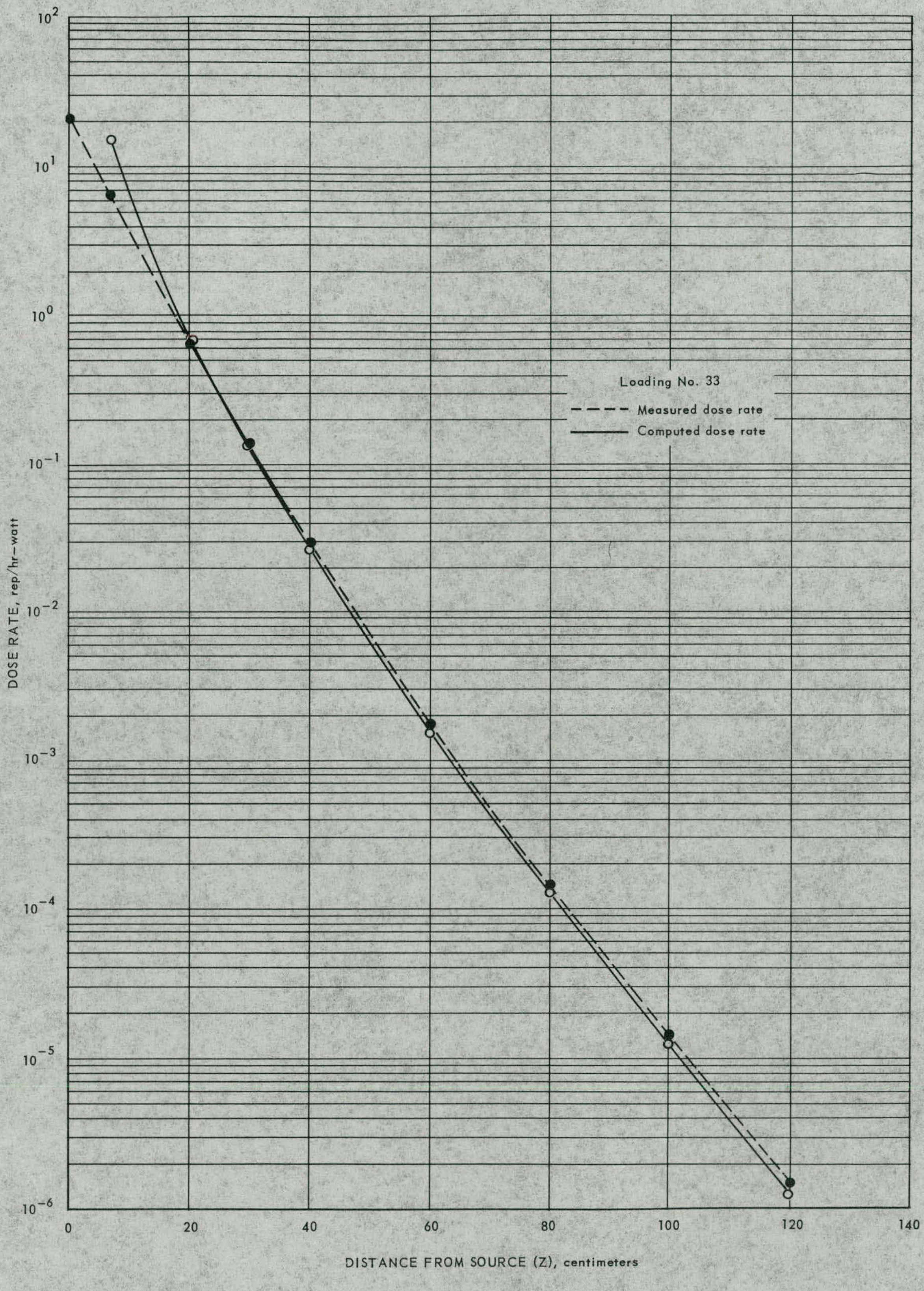

Fig. 6 – Comparison of measured and computed program 04-1 BSR centerline neutron dose rates in water

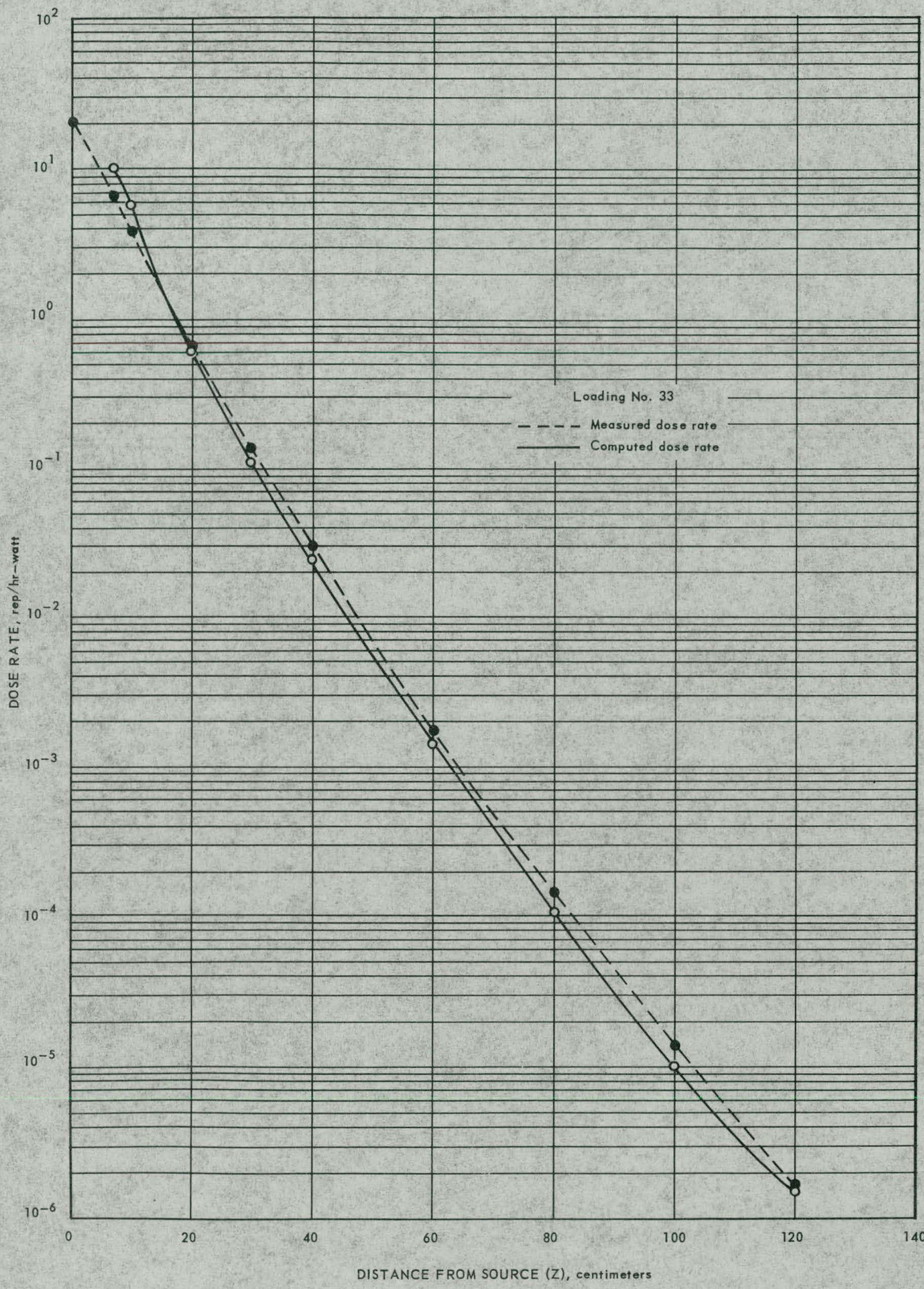

Fig. 7 – Comparison of measured and computed program 14-0 BSR centerline neutron dose rates in water

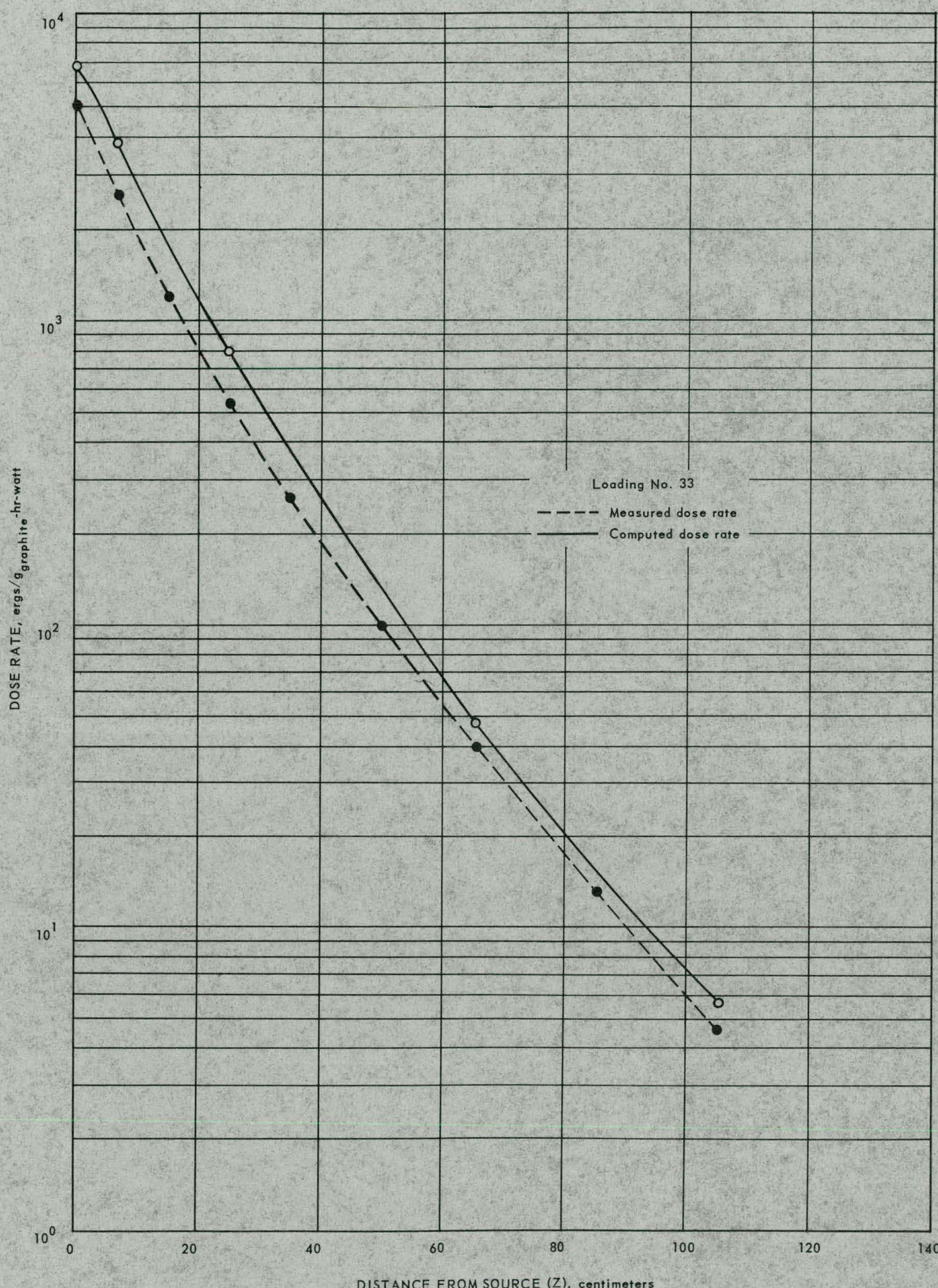

Fig. 8 – Comparison of measured and computed program 04-2 BSR centerline gamma dose rates in water

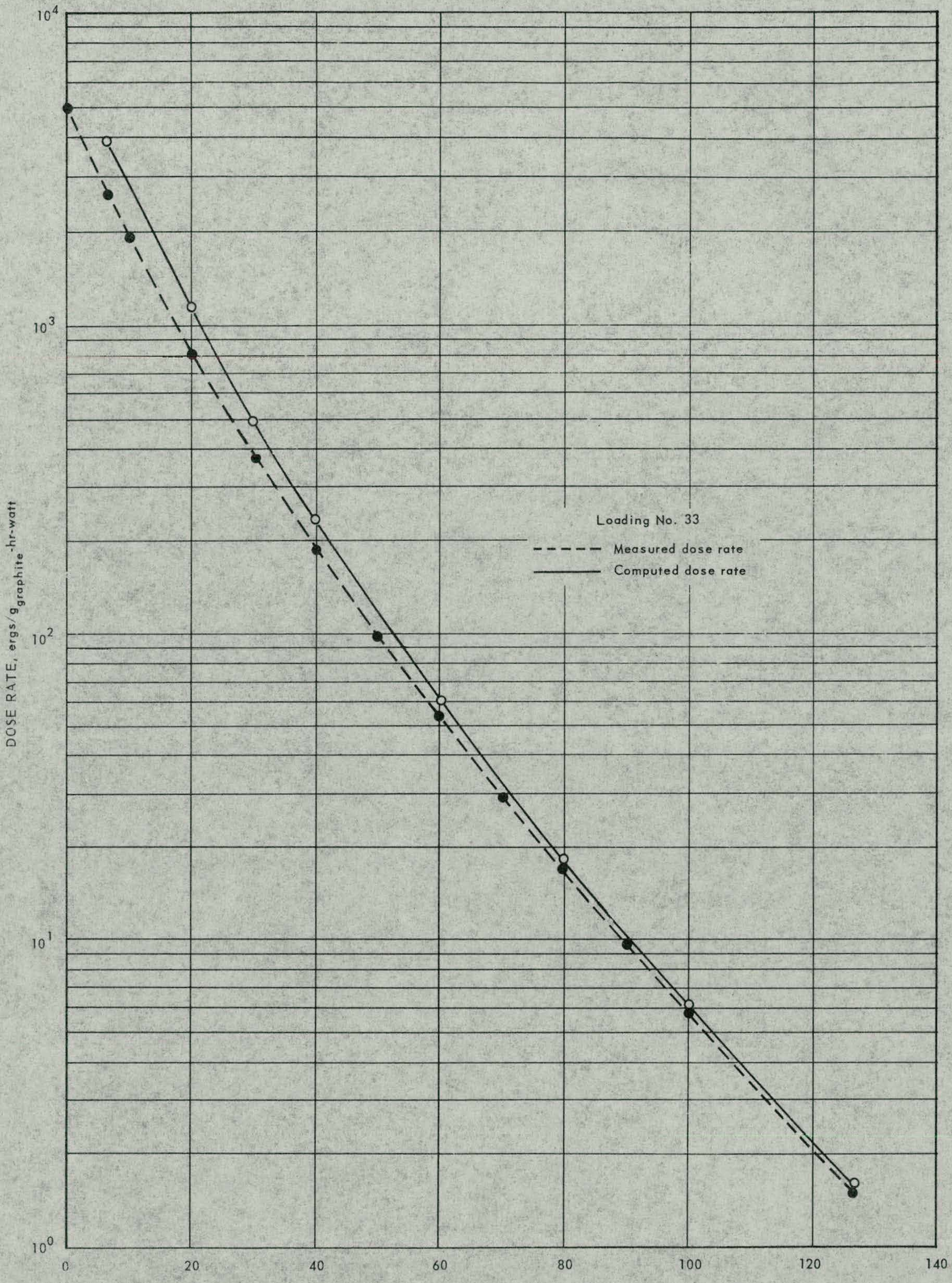

Fig. 9 – Comparison of measured and computed program 04-1 BSR centerline gamma dose rates in water

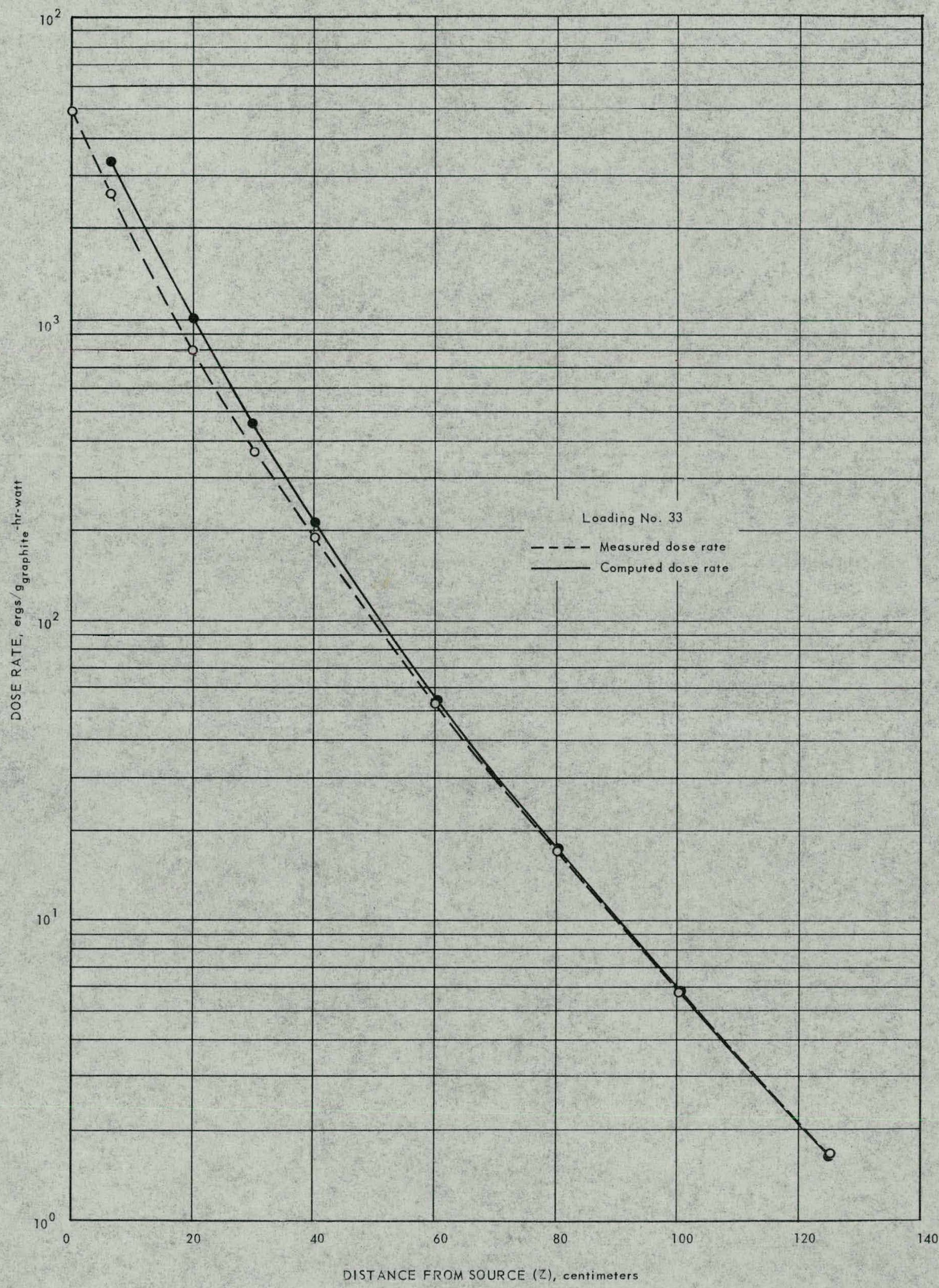

Fig. 10 – Comparison of measured and computed program 14-0 BSR centerline gamma dose rates in water

THIS PAGE

WAS INTENTIONALLY

LEFT BLANK

TABLE 1

POWER DENSITY AT SOURCE POINTS IN ONE-QUARTER CORE FOR PROGRAM 04-1

BSR Loading 33

X, cm	Y, cm	Z, cm	p, watts/cm^3	X, cm	Y, cm	Z, cm	p, watts/cm^3
0	0 and	-23.127	1.13×10^{-5}	0	4.05 and	-23.127	1.055×10^{-5}
0	4.05	-15.418	1.13×10^{-5}	0	12.15	-15.418	1.055×10^{-5}
0	↓	-15.418	9.017×10^{-6}	0	↓	-15.418	1.502×10^{-5}
0		-7.709	9.017×10^{-6}	0		-7.709	1.502×10^{-5}
0		-7.709	8.956×10^{-6}	0		-7.709	1.628×10^{-5}
0		0	8.956×10^{-6}	0		0	1.628×10^{-5}
0		0	1.885×10^{-5}	0		0	8.722×10^{-6}
0		7.709	1.885×10^{-5}	0		7.709	8.722×10^{-6}
0		7.709	1.2904×10^{-5}	0		7.709	1.268×10^{-5}
0		15.418	1.2904×10^{-5}	0		15.418	1.268×10^{-5}
0		15.418	1.208×10^{-5}	0		15.418	1.099×10^{-5}
0	↓	23.127	1.208×10^{-5}	0	↓	23.127	1.099×10^{-5}
0	12.15	-23.127	0	5.08	0 and	-23.127	1.108×10^{-5}
0	and	-15.418	0	5.08	4.05	-15.418	1.108×10^{-5}
0	20.25	-15.418	1.126×10^{-5}	5.08	↓	-15.418	8.834×10^{-6}
0	↓	-7.709	1.126×10^{-5}	5.08		-7.709	8.834×10^{-6}
0		-7.709	1.42×10^{-5}	5.08		-7.709	8.784×10^{-6}
0		0	1.42×10^{-5}	5.08		0	8.784×10^{-6}
0		0	1.477×10^{-5}	5.08		0	1.843×10^{-5}
0		7.709	1.477×10^{-5}	5.08		7.709	1.843×10^{-5}
0		7.709	1.217×10^{-5}	5.08		7.709	1.252×10^{-5}
0		15.418	1.217×10^{-5}	5.08		15.418	1.252×10^{-5}
0		15.418	9.427×10^{-6}	5.08		15.418	1.16×10^{-5}
0	↓	23.127	9.427×10^{-6}	5.08	↓	23.127	1.16×10^{-5}
5.08	4.05 and	-23.127	1.013×10^{-5}	5.08	12.15	-23.127	0
5.08	12.15	-15.418	1.013×10^{-5}	5.08	and	-15.418	0
5.08	↓	-15.418	1.471×10^{-5}	5.08	20.25	-15.418	1.103×10^{-5}
5.08		-7.709	1.471×10^{-5}	5.08	↓	-7.709	1.103×10^{-5}
5.08		-7.709	1.595×10^{-5}	5.08		-7.709	1.377×10^{-5}
5.08		0	1.595×10^{-5}	5.08		0	1.377×10^{-5}
5.08		0	8.455×10^{-6}	5.08		0	1.432×10^{-5}
5.08		7.709	8.455×10^{-6}	5.08		7.709	1.432×10^{-5}
5.08		7.709	1.23×10^{-5}	5.08		7.709	1.193×10^{-5}
5.08		15.418	1.23×10^{-5}	5.08		15.418	1.193×10^{-5}
5.08		15.418	1.055×10^{-5}	5.08		15.418	9.238×10^{-6}
5.08	↓	23.127	1.055×10^{-5}	5.08	↓	23.127	9.238×10^{-6}
10.16	0 and	-23.127	1.017×10^{-5}	10.16	4.05 and	-23.127	8.657×10^{-6}
10.16	4.05	-15.418	1.017×10^{-5}	10.16	12.15	-15.418	8.657×10^{-6}
10.16	↓	-15.418	8.291×10^{-6}	10.16	↓	-15.418	1.367×10^{-5}
10.16		-7.709	8.291×10^{-6}	10.16		-7.709	1.367×10^{-5}
10.16		-7.709	8.241×10^{-6}	10.16		-7.709	1.482×10^{-5}
10.16		0	8.241×10^{-6}	10.16		0	1.482×10^{-5}
10.16		0	1.691×10^{-5}	10.16		0	7.85×10^{-6}
10.16		7.709	1.691×10^{-5}	10.16		7.709	7.85×10^{-6}
10.16		7.709	1.161×10^{-5}	10.16		7.709	1.142×10^{-5}
10.16		15.418	1.161×10^{-5}	10.16		15.418	1.142×10^{-5}
10.16		15.418	1.051×10^{-5}	10.16		15.418	9.566×10^{-6}
10.16	↓	23.127	1.051×10^{-5}	10.16	↓	23.127	9.566×10^{-6}

TABLE 1 (Cont.)

POWER DENSITY AT SOURCE POINTS IN ONE-QUARTER CORE
FOR PROGRAM 04-1

BSR Loading 33

X, cm	Y, cm	Z, cm	p, watts/cm^3	X, cm	Y, cm	Z, cm	p, watts/cm^3
10.16	12.15	-23.127	0	15.24	0 and	-23.127	9.049×10^{-6}
10.16	and	-15.418	0	15.24	4.05	-15.418	9.049×10^{-6}
10.16	20.25	-15.418	1.025×10^{-5}	15.24		-15.418	7.32×10^{-6}
10.16		-7.709	1.025×10^{-5}	15.24		-7.709	7.32×10^{-6}
10.16		-7.709	1.263×10^{-5}	15.24		-7.709	7.206×10^{-6}
10.16		0	1.263×10^{-5}	15.24		0	7.206×10^{-6}
10.16		0	1.329×10^{-5}	15.24		0	1.477×10^{-5}
10.16		7.709	1.329×10^{-5}	15.24		7.709	1.477×10^{-5}
10.16		7.709	1.095×10^{-5}	15.24		7.709	1.017×10^{-5}
10.16		15.418	1.095×10^{-5}	15.24		15.418	1.017×10^{-5}
10.16		15.418	8.481×10^{-6}	15.24		15.418	9.364×10^{-6}
10.16		23.127	8.481×10^{-6}	15.24		23.127	9.364×10^{-6}
15.24	4.05 and	-23.127	6.398×10^{-6}	15.24	12.15 and	-23.127	0
15.24	12.15	-15.418	6.398×10^{-6}	15.24	20.25	-15.418	0
15.24		-15.418	1.184×10^{-5}	15.24		-15.418	8.973×10^{-6}
15.24		-7.709	1.184×10^{-5}	15.24		-7.709	8.973×10^{-6}
15.24		-7.709	1.285×10^{-5}	15.24		-7.709	1.113×10^{-5}
15.24		0	1.285×10^{-5}	15.24		0	1.113×10^{-5}
15.24		0	6.853×10^{-6}	15.24		0	1.153×10^{-5}
15.24		7.709	6.853×10^{-6}	15.24		7.709	1.153×10^{-5}
15.24		7.709	1.011×10^{-5}	15.24		7.709	9.389×10^{-6}
15.24		15.418	1.011×10^{-5}	15.24		15.418	9.389×10^{-6}
15.24		15.418	8.317×10^{-6}	15.24		15.418	7.433×10^{-6}
15.24		23.127	8.317×10^{-6}	15.24		23.127	7.433×10^{-6}
20.32	0 and	-23.127	7.686×10^{-6}	20.32	4.05 and	-23.127	4.644×10^{-6}
20.32	4.05	-15.418	7.686×10^{-6}	20.32	12.15	-15.418	4.644×10^{-6}
20.32		-15.418	6.31×10^{-6}	20.32		-15.418	1.006×10^{-5}
20.32		-7.709	6.31×10^{-6}	20.32		-7.709	1.006×10^{-5}
20.32		-7.709	5.995×10^{-6}	20.32		-7.709	1.042×10^{-5}
20.32		0	5.995×10^{-6}	20.32		0	1.042×10^{-5}
20.32		0	1.225×10^{-5}	20.32		0	5.49×10^{-6}
20.32		7.709	1.225×10^{-5}	20.32		7.709	5.49×10^{-6}
20.32		7.709	8.519×10^{-6}	20.32		7.709	8.241×10^{-6}
20.32		15.418	8.519×10^{-6}	20.32		15.418	8.241×10^{-6}
20.32		15.418	8.455×10^{-6}	20.32		15.418	7.143×10^{-6}
20.32		23.127	8.455×10^{-6}	20.32		23.127	7.143×10^{-6}
20.32	12.15	-23.127	0	25.4	0 and 4.05	-23.127	6.891×10^{-6}
20.32	and	-15.418	0	25.4		-15.418	6.891×10^{-6}
20.32	20.25	-15.418	7.433×10^{-6}	25.4		-15.418	5.048×10^{-6}
20.32		-7.709	7.433×10^{-6}	25.4		-7.709	5.048×10^{-6}
20.32		-7.709	9.086×10^{-6}	25.4		-7.709	4.922×10^{-6}
20.32		0	9.086×10^{-6}	25.4		0	4.922×10^{-6}
20.32		0	9.604×10^{-6}	25.4		0	9.616×10^{-6}
20.32		7.709	9.604×10^{-6}	25.4		7.709	9.616×10^{-6}
20.32		7.709	7.421×10^{-6}	25.4		7.709	7.61×10^{-6}
20.32		15.418	7.421×10^{-6}	25.4		15.418	7.61×10^{-6}
20.32		15.418	5.843×10^{-6}	25.4		15.418	7.85×10^{-6}
20.32		23.127	5.843×10^{-6}	25.4		23.127	7.85×10^{-6}

TABLE 1 (Cont.)

POWER DENSITY AT SOURCE POINTS IN ONE-QUARTER CORE FOR PROGRAM 04-1

BSR Loading 33

X, cm	Y, cm	Z, cm	p, watts/cm^3	X, cm	Y, cm	Z, cm	p, watts/cm^3
25.4	4.05 and	-23.127	3.483×10^{-6}	25.4	12.15 and	-23.127	0
25.4	12.15	-15.418	3.483×10^{-6}	25.4	20.25	-15.418	0
25.4	↓	-15.418	9.011×10^{-6}	25.4	↓	-15.418	6.31×10^{-6}
25.4		-7.709	9.011×10^{-6}	25.4		-7.709	6.31×10^{-6}
25.4		-7.709	8.468×10^{-6}	25.4		-7.709	7.383×10^{-6}
25.4		0	8.468×10^{-6}	25.4		0	7.383×10^{-6}
25.4		0	4.442×10^{-6}	25.4		0	7.383×10^{-6}
25.4		7.709	4.442×10^{-6}	25.4		7.709	7.383×10^{-6}
25.4		7.709	6.348×10^{-6}	25.4		7.709	5.843×10^{-6}
25.4		15.418	6.348×10^{-6}	25.4		15.418	5.843×10^{-6}
25.4		15.418	6.373×10^{-6}	25.4		15.418	4.72×10^{-6}
25.4		23.127	6.373×10^{-6}	25.4		23.127	4.72×10^{-6}
30.48	0 and	-23.127	7.092×10^{-6}	30.48	4.05 and	-23.127	3.508×10^{-6}
30.48	4.05	-15.418	7.092×10^{-6}	30.48	12.15	-15.418	3.508×10^{-6}
30.48	↓	-15.418	5.061×10^{-6}	30.48	↓	-15.418	9.301×10^{-6}
30.48		-7.709	5.061×10^{-6}	30.48		-7.709	9.301×10^{-6}
30.48		-7.709	4.922×10^{-6}	30.48		-7.709	8.607×10^{-6}
30.48		0	4.922×10^{-6}	30.48		0	8.607×10^{-6}
30.48		0	9.591×10^{-6}	30.48		0	4.417×10^{-6}
30.48		7.709	9.591×10^{-6}	30.48		7.709	4.417×10^{-6}
30.48		7.709	7.774×10^{-6}	30.48		7.709	6.26×10^{-6}
30.48		15.418	7.774×10^{-6}	30.48		15.418	6.26×10^{-6}
30.48		15.418	8.089×10^{-6}	30.48		15.418	6.575×10^{-6}
30.48		23.127	8.089×10^{-6}	30.48		23.127	6.575×10^{-6}
30.48	12.15	-23.127	0				
30.48	and	-15.418	0				
30.48	20.25	-15.418	5.995×10^{-6}				
30.48	↓	-7.709	5.995×10^{-6}				
30.48		-7.709	7.08×10^{-6}				
30.48		0	7.08×10^{-6}				
30.48		0	6.79×10^{-6}				
30.48		7.709	6.79×10^{-6}				
30.48		7.709	5.376×10^{-6}				
30.48		15.418	5.376×10^{-6}				
30.48		15.418	4.556×10^{-6}				

TABLE 2

SOURCE DESCRIPTION FOR PROGRAM 14-0

BSR Loading No. 33

Axial Boundary Values

Range 1 Z = - 30.48 to Z = - 22.352 cm
Range 2 Z = - 22.352 to Z = 22.352 cm
Range 3 Z = 22.352 to Z = 30.48 cm

Type 1 - 9 lines

Location:	R, cm	ϕ
	16.2	3.1416
	0	0
	16.2	0
	17.94	3.5857
	11.18	3.9023
	11.18	5.5225
	17.94	5.8391
	17.42	4.2287
	17.42	5.1961

Axial Power Distribution

	$\xi 1$	$\xi 2$	$\xi 3$	$\xi 4$
Range 1	0.3865	-26.42	5.773×10^{-4}	-1.021×10^{-4}
Range 2	0.07028	0	5.773×10^{-4}	3.769×10^{-4}
Range 3	0.3865	26.42	5.773×10^{-4}	-1.021×10^{-4}

Type 2 - 3 lines

Location:	R, cm	ϕ
	15.42	1.5708
	17.94	2.6975
	17.94	0.44415

Axial Power Distribution

	$\xi 1$	$\xi 2$	$\xi 3$	$\xi 4$
Range 1	0.3865	-26.42	4.523×10^{-4}	-7.999×10^{-5}
Range 2	0.07028	0	4.523×10^{-4}	2.953×10^{-4}
Range 3	0.3865	26.42	4.523×10^{-4}	-7.999×10^{-5}

Type 3 - 3 lines

Location:	R, cm	ϕ
	11.18	2.3809
	7.709	1.5708
	11.18	0.76067

TABLE 2 (Cont.)

SOURCE DESCRIPTION FOR PROGRAM 14-0

BSR Loading No. 33

Axial Power Distribution

	$\xi 1$	$\xi 2$	$\xi 3$	$\xi 4$
Range 1	0.3865	-26.42	3.3×10^{-4}	-5.836×10^{-5}
Range 2	0.07028	0	3.3×10^{-4}	2.155×10^{-4}
Range 3	0.3865	26.42	3.3×10^{-4}	-5.836×10^{-5}

All Types

Radial Power Distribution

$\xi 1$	$\xi 2$	$\xi 3$	$\xi 4$
0	0	0	1

TABLE 2 (Cont.)

SOURCE DESCRIPTION FOR PROGRAM 14-0

BSR Loading No. 33

Axial Power Distribution

	ξ 1	ξ 2	ξ 3	ξ 4
Range 1	0.3865	-26.42	4.755×10^{-4}	-8.409×10^{-5}
Range 2	0.07028	0	4.755×10^{-4}	3.104×10^{-4}
Range 3	0.3865	26.42	4.755×10^{-4}	-8.409×10^{-5}

Type 4 - 7 lines

Location:	R, cm	ϕ
	17.42	2.0545
	17.42	1.0871
	22.36	3.9023
	22.36	5.5225
	24.5	4.3756
	23.13	4.7124
	24.5	5.0492

Axial Power Distribution

	ξ 1	ξ 2	ξ 3	ξ 4
Range 1	0.3865	-26.42	4.095×10^{-4}	-7.242×10^{-5}
Range 2	0.07028	0	4.095×10^{-4}	2.674×10^{-4}
Range 3	0.3865	26.42	4.095×10^{-4}	-7.242×10^{-5}

Type 5 - 2 lines

Location:	R, cm	ϕ
	22.36	2.3809
	22.36	0.76067

Axial Power Distribution

	ξ 1	ξ 2	ξ 3	ξ 4
Range 1	0.3865	-26.42	3.513×10^{-4}	-6.214×10^{-5}
Range 2	0.07028	0	3.513×10^{-4}	2.294×10^{-4}
Range 3	0.3865	26.42	3.513×10^{-4}	-6.214×10^{-5}

Type 6 - 4 lines

Location:	R, cm	ϕ
	8.1	3.1416
	8.1	0
	7.709	4.7124
	15.42	4.7124

TABLE 3

GAMMA RAY SOURCE INTENSITY

E, Mev	B, Mev/watt-sec
0.375	9.505×10^{10}
1	9.453×10^{10}
1.5	7.528×10^{10}
2	8.059×10^{10}
2.5	4.167×10^{10}
3	2.972×10^{10}
3.625	2.853×10^{10}
4.5	2.061×10^{10}
5.5	9.33×10^{9}
6.5	5.106×10^{9}
7.5	7.385×10^{9}
8.5	3.069×10^{8}
9.5	5.594×10^{7}
0.5	1.629×10^{11}
1.5	1.697×10^{11}
2.5	8.525×10^{10}
3.5	4.014×10^{10}
4.5	2.024×10^{10}
5.5	1.159×10^{10}
6.5	8.46×10^{9}
7.5	8.59×10^{9}
8.5	3.69×10^{8}
9.5	1.36×10^{8}

TABLE 4

DOSE BUILDUP FOR WATER[a]

E, Mev	B_0	B_1	B_2	B_3
13 Energy Intervals				
0.375	1	1.119	0.6449	0.04602
1	1	0.9396	0.193	-0.002593
1.5	1	0.915	0.09	-0.00146
2	1	0.812	0.0425	-0.00098
2.5	1	0.746	0.016	-0.00049
3	1	0.692	0.0081	-0.00015
3.625	1	0.618	0.0042	-0.0004
4.5	1	0.544	-0.0007	0.00002
5.5	1	0.487	-0.005	0.00011
6.5	1	0.438	-0.0066	0.00013
7.5	1	0.397	-0.0072	0.00016
8.5	1	0.36	-0.0074	0.00018
9.5	1	0.334	-0.0075	0.0002
10 Energy Intervals				
0.5	1	0.849	0.582	0.00988
1.5	1	0.915	0.09	-0.00146
2.5	1	0.746	0.016	-0.00049
3.5	1	0.633	0.0048	-0.00005
4.5	1	0.544	-0.0007	0.00002
5.5	1	0.487	-0.005	0.00011
6.5	1	0.438	-0.0066	0.00013
7.5	1	0.397	-0.0072	0.00016
8.5	1	0.36	-0.0074	0.00018
9.5	1	0.334	-0.0075	0.0002

[a]Reference 3.

TABLE 5

GAMMA RAY LINEAR ABSORPTION CROSS SECTIONS[a]

E, Mev	H_2O Σ, cm^{-1}	Al Σ, cm^{-1}	U Σ, cm^{-1}
0.375	0.109	0.258	5.8
1	0.0706	0.1658	1.416
1.5	0.0576	0.135	1.051
2	0.0493	0.1164	0.9032
2.5	0.0435	0.103	0.842
3	0.0396	0.0953	0.8135
3.625	0.0356	0.088	0.817
4.5	0.0319	0.0788	0.823
5.5	0.029	0.0734	0.86
6.5	0.0268	0.0699	0.898
7.5	0.0251	0.0677	0.935
8.5	0.0235	0.0645	0.954
9.5	0.0224	0.0629	0.972
0.5	0.0962	0.232	3.366
1.5	0.0565	0.135	1.047
2.5	0.0435	0.103	0.842
3.5	0.0361	0.0886	0.804
4.5	0.0319	0.0788	0.823
5.5	0.029	0.0734	0.86
6.5	0.0268	0.0699	0.898
7.5	0.0251	0.0667	0.935
8.5	0.0235	0.0645	0.954
9.5	0.0224	0.0629	0.972

ASSUMED COMPOSITION OF THE BSR

Volume Fractions	
H_2O	0.583
Al	0.415
U	0.002

[a]Reference 4.

TABLE 6

FLUX-TO-DOSE CONVERSION FACTORS

E, Mev	K $\left(\frac{\text{ergs/g of graphite-hr}}{\text{Mev/cm-sec}}\right)$
0.375	1.71×10^{-4}
1	1.62×10^{-4}
1.5	1.47×10^{-4}
2	1.37×10^{-4}
2.5	1.3×10^{-4}
3	1.22×10^{-4}
3.625	1.14×10^{-4}
4.5	1.05×10^{-4}
5.5	9.79×10^{-5}
6.5	9.33×10^{-5}
7.5	9.1×10^{-5}
8.5	8.7×10^{-5}
9.5	8.58×10^{-5}
0.5	1.73×10^{-4}
1.5	1.47×10^{-4}
2.5	1.3×10^{-4}
3.5	1.15×10^{-4}
4.5	1.05×10^{-4}
5.5	9.79×10^{-5}
6.5	9.33×10^{-5}
7.5	9.1×10^{-5}
8.5	8.7×10^{-5}
9.5	8.58×10^{-5}

TABLE 7

THERMAL NEUTRON FLUX DISTRIBUTION USED TO DESCRIBE THE SECONDARY GAMMA SOURCE

	First Axial Distribution
Z, cm	
Z = 0 to 5,	$P_1(Z) = 1.127 \times 10^7 \cos - 0.31416\ (Z - 2.5) + 3.03 \times 10^6$
Z = 5 to 30,	$P_2(Z) = 3.391 \times 10^7 \exp - 0.2061\ Z$
Z = 30 to 60,	$P_3(Z) = 8.712 \times 10^6 \exp - 0.16276\ Z$
Z = 60 to 100,	$P_4(Z) = 5 \times 10^2 \exp - 0.12749\ (Z - 60)$
	Radial Distribution[a]
r, cm	
r = 0 to 5.08,	$P_1(r) = 1 \exp 0 \cdot r$
r = 5.08 to 22.86,	$P_2(r) = 1.264 \exp -0.04617\ r$
r = 22.86 to 50.8,	$P_3(r) = 3.264 \exp - 0.08766\ r$
r = 50.8 to 60.96,	$P_4(r) = 126.8 \exp - 0.1597\ r$
	Second Axial Distribution
Z, cm	
Z = 100 to 170,	$P_1(Z) = 2.826 \exp - 0.10738\ (Z - 100)$
Z = 170 to 200,	$P_2(Z) = 1.541 \times 10^{-3} \exp - 0.070642\ (Z - 170)$
Z = 200 to 250,	$P_3(Z) = 1.902 \times 10^{-4} \exp - 0.039616\ (Z - 200)$
Z = 250 to 400,	$P_4(Z) = 2.5177 \times 10^{-5} \exp - 0.029793\ (Z - 250)$

[a]The radial distribution is the same in both cases.

THIS PAGE

WAS INTENTIONALLY

LEFT BLANK

References

1. "Attenuation in Water of Radiation from the Bulk Shielding Reactor; Measurement of Gamma Ray Dose Rate, Fast Neutron Dose Rate, and Thermal Neutron Flux," prepared by the staff of the Bulk Shielding Reactor, Oak Ridge National Laboratory, ORNL-2518.

2. Johnson, E. B., "Power Calibration for BSR Loading 33," CF 57-11-30, November 28, 1957.

3. Goldstein, Herbert; Wilkins, J. Ernest, Jr., "Calculations of the Penetration of Gamma Rays," NYO-3075, June 30, 1954.

4. Grodstein, Gladys White, "X-Ray Attenuation Coefficients from 10 Kev to 100 Mev," NBS Circular 583, April 30, 1957.

5. Moteff, John, "Miscellaneous Data for Shielding Calculations," General Electric Company, Aircraft Nuclear Propulsion Department, APEX-176, December 1, 1954.

6. Capo, M. A.; Edwards, W. E.; Loechler, J. J.; and Paine, K. A.; "Shielding Computer Program 04-4, Reactor Shield Analysis," General Electric Company, Aircraft Nuclear Propulsion Department, XDC 59-7-150, July 22, 1959.